WWW.IJRPR.COM

International Journal of Research Publication and Reviews

Journal homepage: www.ijrpr.com ISSN 2582-7421

Numerical Simulation and Modeling of Nontoxic Perovskite Solar Cell Based on $CH_3NH_3SnI_3$ with TiO_2 as ETL and $CuSbS_2$ as HTL

Alok Singh Kushwaha [a], Alok Agarwal [b], Aasha Chauhan [c], Megha Dewan [d]

[a,b,c,d] *Aravali College of Engineering amd Management, Faridabad, Haryana 121102, India*

DOI: https://doi.org/10.55248/gengpi.5.0324.0609

A B S T R A C T

Lead halide perovskite based solar cell have gained much attention among researcher due to its high power conversion efficiency of over 23%.The most performing solar cell uses lead salt, which are highly toxic material thereby can pollute the environment with bad impact on human health. The consequences related to organic and inorganic lead salts perovskite is under debate. In this study we focused on lead free substitute, CH3NH3SnI3 light absorbing material for designing solar cell with TiO2 as electron transport layer and CuSbS2 as Hole Transport Layer

The numerical simulation is done with two proposed device with different HTL material. The choice of HTL material can significantly influence the charge transport properties, interface characteristics, and overall device performance. By modeling the devices using computational tools such as SCAPS (Solar Cell Capacitance Simulator), various performance parameters such as efficiency, fill factor, and current-voltage characteristics is analysed and compared with previous literature work. In our initial simulated results, device achieves the best efficiency of 29.39% with JSC = 33.500115mAcm−2, VOC = 1.0493V, and FF = 83.60%. Subsequently, we have analysed the impact of thickness on the recombination rate of charge carriers in the perovskite absorber layer

Keywords: Perovskite solar cell, $CuSbS_2$, Scaps 1D

1. Introduction

Conventional sources of energy are formed form natural process and non-conventional sources are harnessed form natural sources. Fossil fuels have numerous adverse effects on the environment, contributing significantly to climate change and various forms of pollution. Fossil fuel combustion emits pollutants such as sulfur dioxide (SO2), nitrogen oxides (NOx), particulate matter (PM), and volatile organic compounds (VOCs). These pollutants contribute to smog, acid rain, respiratory diseases, and other health issues. Climate change driven by fossil fuel emissions is causing shifts in ecosystems and habitats, leading to loss of biodiversity and increased risk of extinction for many plant and animal species. Due to this Solar energy now becomes a leading source for obtaining green energy.[1] Lead-based perovskite solar cells are prone to degradation when exposed to moisture, heat, or light and also bears toxic nature.[2] Tin-based perovskite solar cells offer improved stability under various environmental conditions, making them potentially longer-lasting. Tin-based perovskite materials have demonstrated a wider range of absorption across the visible spectrum compared to lead-based counterparts.[3] This characteristic allows for more efficient utilization of sunlight, potentially leading to higher power conversion efficiency. Recombination leads to the loss of charge carriers (electrons and holes) within the solar cell, which reduces overall efficiency. Tin-based perovskite materials have shown lower rates of recombination compared to lead-based materials, resulting in improved device performance.[4] These advantages make tin-based perovskite solar cells an attractive option for next-generation photovoltaic technology. However, there are still challenges to address, such as scalability, cost-effectiveness, and large-scale production, before these cells can be widely commercialized.[5] Ongoing research aims to overcome these hurdles and further enhance the performance and stability of tin-based perovskite solar cells. A conventional perovskite cell comprises of perovskite based light harvesting material assimilated in between ETL & HTL. There has been many articles reported the viability of tin based perovskite solar cell. It has better stability, wider range of coverage of visible spectrum and low recombination rate than lead perovskite solar cell

2. Device structure and computation

In this study, the device simulator, the Solar Cell Capacitance Simulator (SCAPS) 27 developed by University of Gent, was used to model the perovskite solar cells. The proposed solar cell consists of transparent conductive oxide (TCO)/buffer/absorber/hole transport material (HTM). Common substrate materials include glass, flexible plastics, or metal foils. The transparent conductive oxide (TCO) electrodes, such as fluorine-doped tin oxide (FTO) or indium tin oxide (ITO), are deposited onto the substrate. These electrodes will serve as the front contact for the solar cell, allowing light to enter. The perovskite layer is typically deposited using solution processing techniques such as spin-coating, doctor-blading, or spray-coating.[6] The precursor solution, containing the necessary metal halide salts (e.g., lead or tin halides) and organic components (e.g., methylammonium iodide, formamidinium

iodide), is deposited onto the substrate and then annealed to form the perovskite crystal structure. Common HTL materials include organic small molecules such as spiro-OMeTAD (2,2',7,7'-tetrakis(N,N-di-p-methoxyphenylamine)-9,9'-spirobifluorene) or polymer-based materials. The HTL facilitates the extraction of positive charge carriers (holes) from the perovskite layer. Finally, a back electrode is deposited onto the HTL. This electrode typically consists of a metal layer such as gold, silver, or aluminum. The back electrode serves as the contact for the negative charge carriers (electrons) and completes the electrical circuit of the solar cell. The solar cell devices undergo characterization and testing to evaluate their performance parameters, including efficiency, stability, and durability. Various analytical techniques, such as current-voltage (I-V) measurements, spectral response measurements, and accelerated aging tests, are performed to assess the device performance. Numerical simulations are used to model the fundamental physical processes that govern solar cell operation, such as light absorption, carrier generation, recombination, and transport. These simulations often employ semiconductor device physics equations, such as the drift-diffusion equations or the Schrödinger equation for quantum mechanical effects in nanoscale devices. Numerical simulations are used to investigate the influence of material properties (e.g., bandgap, mobility, doping concentration) and interfaces (e.g., heterojunctions, contacts) on solar cell performance. Numerical simulations are employed for optimizing solar cell designs to achieve higher efficiency, improved stability, and reduced manufacturing costs. Parametric studies, sensitivity analyses, and optimization algorithms are used to explore the design space and identify optimal device configurations

2.1 Table 1 - Input parameters used in simulation.

Parameters	CuSbS2 [HTL] [7]	SpiroOMeTAD [HTL][8]	$CH_3NH_3SnI_3$[7]	TiO_2[ETL]	FTO
Thickness(nm)	400	350	100-600	350	200
Bandgap (eV)	1.58	3.17	1.3	3.2	3.5
Electron affinity (eV)	4.2	2.6	4.2	4.1	4
Dielectric permittivity (relative)	14.6	3	10	9	9
CB effective density of states ($1/cm^3$)	$2\ x10^{18}$	$2.2\ x10^{18}$	$1\ x10^{18}$	$2.2\ x10^{18}$	$2\ x10^{18}$
VB effective density of states ($1/cm^3$)	$1\ x10^{19}$	$1.8\ x10^{19}$	$1\ x10^{18}$	$1\ x10^{19}$	$1.8\ x10^{19}$
Electron thermal velocity (cm/s)	$1\ x10^{7}$	$1\ x10^{7}$	$1\ x10^{7}$	$1\ x10^{7}$	$1\ x10^{7}$
Hole thermal velocity (cm/s)	$1\ x10^{7}$	$1\ x10^{7}$	$1\ x10^{7}$	$1\ x10^{7}$	$1\ x10^{7}$
Electron mobility (cm^2/Vs)	49	$2\ x10^{-4}$	1.6	20	20
Hole mobility (cm^2/Vs)	49	$2\ x10^{-4}$	1.6	10	10
Shallow uniform donor density ND ($1/cm^3$)	0	0	0	$1\ x10^{18}$	$2\ x10^{19}$
Shallow uniform acceptor density NA ($1/cm^3$)	$1.38\ x10^{18}$	$2\ x10^{19}$	$3.2\ x10^{15}$	0	0
N_t Total ($1/cm^3$)	$1\ x10^{14}$	$1\ x10^{14}$	$1\ x10^{14}$	$1\ x10^{15}$	$1\ x10^{15}$

3. Simulation Methodology and Device structure

Now a days number of open source modelling and simulation tools are available to study the performance of PSCs such as AFORS HET, SCAPS and PC 1D. In this study, we used a SCAPS 1D (3.3.09) simulation tool, developed by Marc Burgelman and his team at Department of Electronics and Information Systems, University of Gent, Belgium. Poisson and continuity equation are basic building block of the Solar Cell Capacitance Simulator (SCAPS), one dimensional simulation programme. Poisson equation is used for computation of electric filed while continuity equation is used to study the transportation of electron-hole charges. The proposed planar heterojunction n-i-p structure, Glass/FTO/TiO_2/$CH_3NH_3SnI_3$/HTL simulated under AM 1.5 G sun spectra at room temperature (300K) with illumination intensity of 1000 W/m^2.Figure 1 shows the proposed device configuration.All the necessary parameters that are required for performance analysis of this solar cell, is collected from the previous, experimental and theoretical studies done by various researchers and mentioned in Table 1.

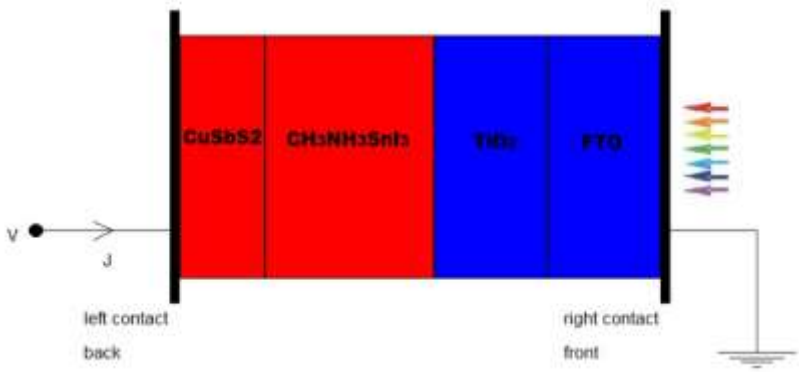

Fig.1 Proposed solar cell configuration

3.1 Standard boundary Conditions

The drift-diffusion current equations are derived from the moments of Boltzmann transport equation (BTE). The continuity equations are the conservation laws for the charge carriers, which are derived taking the zeroth moment of BTE. The complete drift-diffusion model is based on the following set of equations in 1D.The drift-diffusion current expressions for electrons and holes is given by: *Current equations*

$$J_n = \quad qn(x)\mu_n E(x) + qD_n \frac{dn}{dx} \tag{1}$$

$$J_p = qn(x)\mu_p E(x) - qD_p \frac{dp}{dx}, \tag{2}$$

D is diffusion coefficient, q is the absolute value of the electronic charge. The perovskite $CH_3NH_3SnI_3$ is sandwiched between HTL and ETL which creates excess of holes at one and excess of electrons at other boundary. The electrons and holes moves from higher concentration to lower concentration and give rise to diffusion current .The electric field from ETL region to HTL region give rise drift current. The effect of drift and diffusion current provides current density given by eq. (1) & (2).

Continuity equations

$$\frac{\partial n}{\partial t} = \frac{1}{q} \mathrm{n\ J_n} + \mathrm{U_n} \tag{3}$$

$$\frac{\partial n}{\partial t} = \frac{1}{q} \mathrm{n\ J_p} + \mathrm{U_p} \tag{4}$$

U_n and U_p are the net generation-recombination rates.

Poisson's equation

$$-\nabla^2 \Psi = \frac{dE}{dx} = \frac{\rho}{\varepsilon} \tag{5}$$

$$\rho = q\ (p\text{-}n+N_D^+\text{-}N_A^-) \tag{6}$$

$$\nabla^2 \Psi = \frac{q}{\varepsilon} (n\text{-}p+N_A^+\text{-}N_D^-) \tag{7}$$

Ψ is the electrostatic potential,ϵ *is* material's permittivity ,E is electric field, ρ is charge density According to eq.5 a higher change in the electric field relative to position in a given material signifies a higher charge density. In our design, Glass/FTO/ETL/ $CH_3NH_3SnI_3$ /HTL, according to Poisson's equation, electric field varies with thickness of $CH_3NH_3SnI_3$. The perovskite is simulated for thickness 100 nm $\leq (t_0) \geq$ 600 nm. Due the presence of holes at the interface HTL/ $CH_3NH_3SnI_3$ boundary, electric potential $\nabla^2\Psi$ is high due to holes similarly at the interface ETL/ $CH_3NH_3SnI_3$ have high electric potential due to higher electron concentration. Hence there is gradient variation in electric potential.

3.2 Performance Parameter

The solar cell performance is evaluated on the basis of certain parameter i.e. the peak power (P_{max}), the open circuit Voltage (V_{oc}),the short circuit current density (J_{sc}),the fill factor (FF) ,the performance conversion efficiency (η), the quantum efficiency (QE) etc.[9] Under standard test condition, solar cell absorbs the energy of group of photons, incident on it, from the sunlight. This results in the generation of electron-hole pairs, which starts moving towards opposite electrode. At the p-n junction net current (J_j) is due to the reverse current (J_o) and light induced recombination current (J_r). The relation between J_o and J_r is given by equation

$$J_r = J_o \exp(qV/kT) \tag{8}$$

$$J_j = J_r - J_o \tag{9}$$

$$J_j = J_o [(\exp(qV/kT)-1] \tag{10}$$

If the load R_L is connected between the anode and cathode, the J_L current is observed in the path, which is due to movement of electrons externally. There is another current at the junction due to internal movement of electrons. These currents are the function of solar cell area, hence there is a need to analyse current per area ($J=I/A$).

$$J_l = J_{sc} - J_j \tag{11}$$

$$J_l = J_{sc} - J_o [(\exp(qV/kT)-1] \tag{12}$$

When external path is open ($J_l = 0$), $V=V_{oc}$ (open circuit voltage), from eq. (12),the expression for V_{oc} given by

$$\frac{kT}{q} \ln\left(\frac{J_{sc}}{J_o}+1\right) \tag{13}$$

When (V = 0), Jl = J_{sc} (short circuit current), $\frac{kT}{q}$ is thermal voltage Jsc inversely proportional to the band gap (E_g).The power from the solar cell is zero at Jsc and Voc . Fill factor (FF) is used to determine maximum power from the solar cell. Performance of cell is directly proportional to fill factor and inversely proportional to band gap (E_g) of the absorber layer. It is measured as ratio of maximum power from solar cell to the product of J_{sc} and V_{oc} The efficiency of solar cell is determined by the fraction of incident power which is converted to electricity. It is ratio of obtained maximum power (P_{max}) to incident power (P_{in}).

$$PCE = \left(\frac{P_{max}}{P_{in}}\right) x100 \quad (14)$$

$$P_{max} = V_{oc}\, I_{sc}\, FF \quad (15)$$

$$P_{in}=1\text{kW/m}^2 \quad (16)$$

The "*quantum efficiency*" (*Q.E.*) is the ratio of the number of carriers collected by the solar cell to the number of photons of a given energy incident on the solar cell. The quantum efficiency is zero for photons with energy below the band gap of absorber. If the energy of photons is below the band gap of absorber, than QE is zero.

4 Results and Discussion

Various parameters collected from authenticated previous research are listed in Table 1. SCAPS 1D simulation tool is utilized to analyze the performance parameters of CH3NH3SnI3-based solar cells with different device configurations. The results obtained from this study are compared with relevant previous work in this field, as presented in Table 2.

4.1 Optimization of absorber layer thickness:

Exploring perovskite materials with enhanced optoelectronic properties and alternative device architectures is crucial for advancing solar cell performance. The light absorber material is where the generation, recombination, and transportation of charge carriers occur. Studies in the literature indicate that variations in the active layer can significantly impact carrier lifetime and diffusion, thus affecting overall performance. Optimizing the thickness of the perovskite layer is one way to enhance solar cell performance. $CH_3NH_3SnI_3$ possesses a suitable bandgap for absorbing sunlight, making it an effective light absorber in solar cells. Its bandgap can be tuned by adjusting the chemical composition or through structural modifications. It exhibits a high absorption coefficient across a broad range of wavelengths, enabling efficient harvesting of solar radiation. The optical and electronic properties of $CH_3NH_3SnI_3$ can be tuned by controlling factors such as the stoichiometry, crystal structure, and morphology of the material. This tunability offers flexibility in optimizing the absorption spectrum and charge transport characteristics for solar cell applications. Studies have shown that $CH_3NH_3SnI_3$ can exhibit long carrier diffusion lengths and lifetimes, indicating efficient charge carrier generation and transport within the material. These properties are essential for achieving high-performance solar cells with minimal charge recombination losses. The performance of cell is investigated by varying the perovskite thickness (100-600 nm)

4.2 Investigation of different HTL materials on device performance

We investigate the effect of HTL $CuSbS_2$ and Spiro-OMeTAD in our proposed designed. $CuSbS_2$ exhibits a high absorption coefficient, allowing it to efficiently absorb sunlight and facilitate the generation of charge carriers. It demonstrates good thermal stability, enabling to withstand elevated temperatures during device fabrication processes and operation, thus ensuring the durability of the solar cell. $CuSbS_2$ possesses a bandgap suitable for absorbing a portion of the solar spectrum, making it compatible with solar cell applications. Its bandgap can be tailored through compositional engineering for optimized light absorption. Copper, antimony, and sulphur, the constituent elements of CuSbS2, are abundant in nature, which contributes to the material's potential for large-scale production and cost-effectiveness in solar cell manufacturing. Overall, these properties make $CuSbS_2$ a promising candidate for use as a hole transport layer in solar cells, contributing to the efficiency and stability of the devices. Spiro-OMeTAD possesses excellent hole transport properties, making it well-suited for efficiently transporting positive charges (holes) within the device structure. Spiro-OMeTAD exhibits high hole mobility, facilitating the rapid and efficient movement of charge carriers through the material. This property is crucial for minimizing charge recombination losses and enhancing device performance. Spiro-OMeTAD is known for its stability under ambient conditions, which is essential for ensuring the long-term reliability and durability of solar cell devices. It is compatible with various photoactive materials, including perovskites and organic semiconductors, making it a versatile choice for hole transport layers in different types of solar cells. In our finding , $CuSbS_2$ as HTL shows high efficiency compared to Spiro-OMeTAD

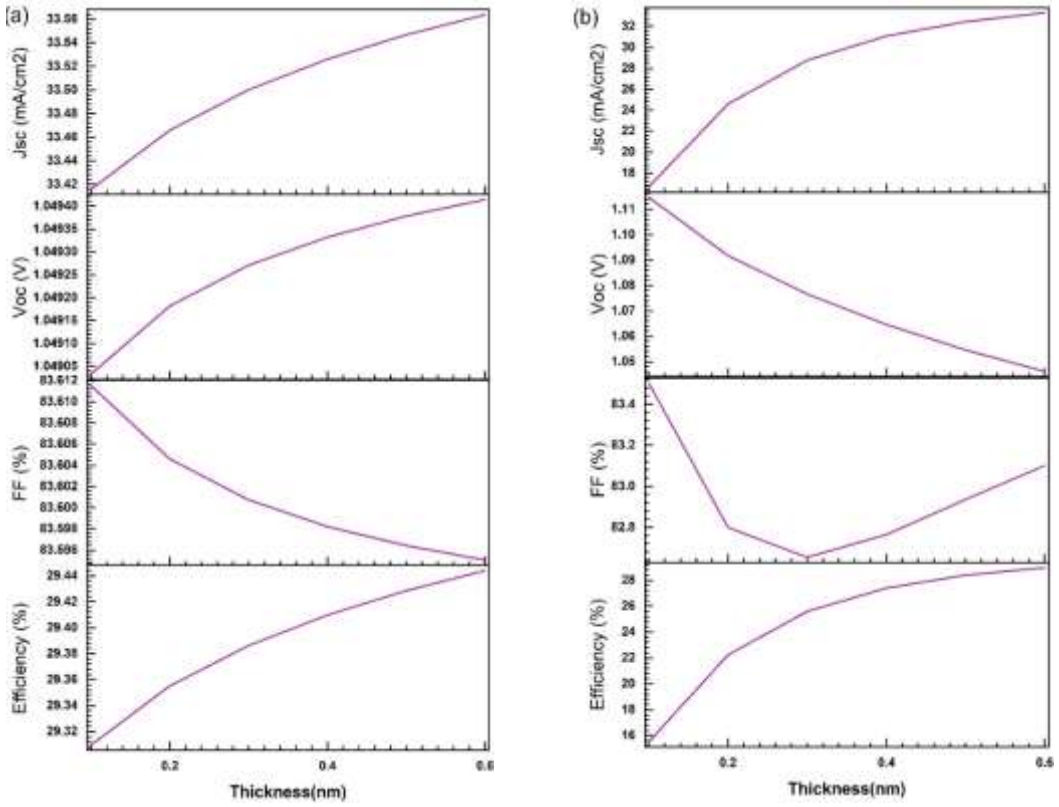

Fig *(a*) performance of PSC with variation of active material thickness with HTL $CuSbS_2$ (b) performance of PSC with variation active material thickness with HTL Spiro-OMeTAD

Table 2 – Parameter obtained with different HTL

Proposed Designs	**Efficiency (*η*) (%)**	**FF(%)**	**Voc(V)**	**J_{SC} ($mAcm^{-2}$)**	**Reference**
Glass/FTO/ TiO_2/ $CH_3NH_3SnI_3$ / $CuSbS_2$	29.39	83.60	1.0493	33.500115	This work
Glass/FTO/ TiO_2/ $CH_3NH_3SnI_3$ / SpiroOMeTAD	28.97	83.10	1.0461	33.319953	This work
FTO/TiO2/$CH_3NH_3SnI_3$/SpiroOMeTA	23.36	79.99	0.92	10.11	[10]
FTO/TiO2/CH3NH3SnI3/CuI [11]	20.35	76.94	0.84	31.38	[11]

4. Conclusion

One of the advantages of $CH_3NH_3SnI_3$ is that it contains tin (Sn) instead of lead (Pb), making it a lead-free alternative to traditional perovskite materials such as $CH_3NH_3PbI_3$. This is significant for addressing environmental and health concerns associated with lead-based materials.In this paper, the solar cell capacitance simulator SCAPS-1D tool has been used to perform the numerical simulation on Perovskite Solar Cell. The structure of the device consists of materials FTO/TiO_2/ $CH_3NH_3SnI_3$/$CuSbS_2$/Au. The effect of different absorber parameters such as thickness, defect density, valence band density of states, and device operating conditions have been thoroughly examined. A thickness of 0.6 µm is found to be optimal for achieving 29.39 % efficiency. The absorber layer ($CH_3NH_3SnI_3$) thickness and defect density have the greatest influence on the Perovskite cell efficiency (PCE). The obtained optimal parameters are V_{oc} = 1.0409 V, J_{sc} = 33.88 mA/cm^2 , FF = 84.31%, and PCE = 29.74%. Based on the results, it is clearly shown that eco-friendly lead-free Perovskite solar cells are a potential candidate for fabricating solar cell and its possibility for the commercialization. Overall, $CH_3NH_3SnI_3$ shows promise as a light-absorbing material for solar cell applications, offering high absorption coefficients, tunable properties, and the potential for lead-free alternatives. Ongoing research efforts are focused on further improving its efficiency, stability, and scalability for commercial deployment in photovoltaic devices

References

[1] S. Sharma, K. K. Jain, and A. Sharma, “Solar Cells: In Research and Applications—A Review,” Mater. Sci. Appl., vol. 06, no. 12, pp. 1145–1155, 2015, doi: 10.4236/msa.2015.612113.

[2] M. Kumar, A. Raj, A. Kumar, and A. Anshul, "An optimized lead-free formamidinium Sn-based perovskite solar cell design for high power conversion efficiency by SCAPS simulation," Opt. Mater. (Amst)., vol. 108, no. August, p. 110213, 2020, doi: 10.1016/j.optmat.2020.110213.

[3] Z. Dai et al., "Stable tin perovskite solar cells enabled by widening the time window for crystallization," Sci. China Mater., vol. 64, no. 8, pp. 1849–1857, 2021, doi: 10.1007/s40843-020-1581-4.

[4] S. S. Hussain et al., "Numerical Modeling and Optimization of Lead-Free Hybrid Double Perovskite Solar Cell by Using SCAPS-1D," J. Renew. Energy, vol. 2021, pp. 1–12, 2021, doi: 10.1155/2021/6668687.

[5] K. Deepthi Jayan and V. Sebastian, "Comprehensive device modelling and performance analysis of MASnI3 based perovskite solar cells with diverse ETM, HTM and back metal contacts," Sol. Energy, vol. 217, pp. 40–48, Mar. 2021, doi: 10.1016/j.solener.2021.01.058.

[6] D. Sharma, R. Mehra, and B. Raj, "Optimization of tin based perovskite solar cell employing CuSbS2 as HTL: A numerical simulation approach," Opt. Mater. (Amst)., vol. 134, no. October, 2022, doi: 10.1016/j.optmat.2022.113060.

[7] K. Kumari, A. Jana, A. Dey, T. Chakrabarti, and S. K. Sarkar, "Lead free CH3NH3SnI3 based perovskite solar cell using ZnTe nano flowers as hole transport layer," Opt. Mater. (Amst)., vol. 111, no. August 2020, pp. 1–7, 2021, doi: 10.1016/j.optmat.2020.110574.

[8] N. J. Valeti, K. Prakash, and M. K. Singha, "Numerical simulation and optimization of lead free CH3NH3SnI3 perovskite solar cell with CuSbS2 as HTL using SCAPS 1D," Results Opt., vol. 12, no. April, pp. 1–10, 2023, doi: 10.1016/j.rio.2023.100440.

[9] K. Kumar and P. Giri, "Planar heterojunction formamidinium lead-based perovskite solar cells with MXenes/Au electrode," Opt. Quantum Electron., vol. 55, no. 8, 2023, doi: 10.1007/s11082-023-05024-z.

[10] J. Catalan, K. Fu, Q. Zhou, and Y. Chen, "Device simulation of lead-free CH 3 NH 3 SnI 3 perovskite solar cells with high efficiency Device simulation of lead-free CH 3 NH 3 SnI 3 perovskite solar cells with high efficiency ∗," 2016, doi: 10.1088/1674-1056/25/10/108802.

[11] E. Danladi, A. O. Salawu, M. O. Abdulmalik, and D. Emmanuel, "Optimization of Absorber and ETM Layer Thickness for Enhanced Tin based Perovskite Solar Cell Performance using SCAPS-1D Software," no. May, 2022, doi: 10.47514/phyaccess.2022.2.1.001.